

# Effect of Temporal Correlation in the Presence of Spatial Correlation on Interference Suppression

Rizwan Ghaffar, Raymond Knopp  
Eurecom, 2229 route des Crêtes B.P.193  
06904 Sophia Antipolis Cedex FRANCE

Email: rizwan.ghaffar@eurecom.fr, raymond.knopp@eurecom.fr

**Abstract**—In this paper, we look at the combined effect of spatial and temporal correlation on low complexity max log MAP detector in the scenario of interference suppression. Since the max log MAP criteria is not directly related to the error probability, it is of considerable interest to study the error probability performance of this detector in practical scenario of correlated fading. We consider narrowband MIMO channel which experiences spatially and temporally correlated wide-sense stationary Rayleigh fading. Employing *moment generating function* (MGF)-based approach, we derive upper bounds of coded pairwise error probability (PEP) and study the effect of spatial and temporal correlation in the presence of non Gaussian interference. Analytical results are then validated by simulations which demonstrate that low complexity max log MAP detector is not only characterised by full diversity but the degrading effect of temporal and spatial correlation is also less pronounced on this detector as compared to other linear detectors as MMSE.

**Keywords**—Interference suppression, Max log MAP detector, Pair wise error probability analysis, Spatial correlation, Temporal correlation.

## I. INTRODUCTION

The objective of achieving higher spectral efficiency in the upcoming wireless standards as 3GPP LTE [1] is leading to the employment of multi-element antenna arrays (MEA) at the mobile station (MS) in addition to existing multi antenna base stations (BSs) thereby leading to a MIMO system. The same aspiration is advocating the frequency reuse factor of one in future mobile systems [1] but that would lead to an interference limited system. To efficiently exploit these spatial dimensions, researchers are focusing on interference alignment, interference mitigation and interference suppression to diminish, manage or exploit these interferers. In this paper, we focus on interference suppression and carry out the performance analysis of low complexity max log MAP detector [2] for narrowband bit interleaved coded modulation (BICM) [3] MIMO based cellular system.

For performance analysis, naive assumption of independent and identically distributed (iid) fading channel may not be true in most of the real world scenarios [4]. The gains of interference suppression are sensitive to the presence of spatial and temporal correlation introduced by the radio environment. For a narrowband MIMO wireless system in the real world, subchannels of a MIMO wireless system have both transmit and receive spatial correlation and the fading of each subchannel has temporal correlation.

In this paper, we investigate the effects of mobile station (MS) and base station (BS) antennas correlation combined with the temporal correlation in the presence of one strong interference on coded pairwise error probability (PEP) of the low complexity max log MAP detector. Using the *moment generating function* (MGF) approach associated with the quadratic form of a complex Gaussian random variable, we derive analytical expressions for upper bounds on coded PEP of low complexity max log MAP detector. We demonstrate the strength of our new analytical PEP upper bounds by simulating the performance of a MS in the presence of one interferer of varying strength and rate using the low complexity max log MAP detector and linear MMSE detector.

Regarding notations, we will use lowercase or uppercase letters for scalars, lowercase boldface letters for vectors and uppercase boldface letters for matrices.  $(\cdot)^T$ ,  $(\cdot)^*$  and  $(\cdot)^\dagger$  indicate transpose, conjugate and conjugate transpose operations respectively.  $|\cdot|$  and  $\|\cdot\|$  indicate norm of scalar and vector while  $abs(\cdot)$  denotes absolute value. The notation  $E(\cdot)$  denotes the mathematical expectation while  $Q(y) = \frac{1}{\sqrt{2\pi}} \int_y^\infty e^{-x^2/2} dx$  denotes the Gaussian Q-function.  $\mathbf{A}_{M \times N}$  indicates a matrix  $\mathbf{A}$  with  $M$  rows and  $N$  columns whereas  $\text{vec}(\mathbf{A})$  denotes the vectorization operator which stacks the columns of  $\mathbf{A}$ . The matrix  $\mathbf{I}_n$  is the  $n \times n$  identity matrix and the element at the  $i$ -th row and  $j$ -th column of matrix  $\mathbf{A}$  is denoted as  $\mathbf{A}(i, j)$ .

The paper is divided into five sections. In section II, we define the system model, while section III discusses the PEP analysis of low complexity max log MAP detector. Section IV contains the simulation results which is followed by the conclusions.

## II. SYSTEM MODEL

We consider the downlink of a narrowband single frequency reuse cellular system with  $n_r$  antennas at the MS. We assume that two spatial streams from two BSs arrive at the MS as  $\mathbf{x}_1$  (desired stream) and  $\mathbf{x}_2$  (interference stream).  $x_1$  is the symbol of  $\mathbf{x}_1$  over a signal set  $\chi_1$  and  $x_2$  is the symbol of  $\mathbf{x}_2$  over signal set  $\chi_2$ . During the transmission at BS-1, code sequence  $\mathbf{c}_1$  is interleaved by  $\pi_1$  and then is mapped onto the signal sequence  $\mathbf{x}_1 \in \chi_1$ . Bit interleaver for the first stream can be modeled as  $\pi_1 : k' \rightarrow (k, i)$  where  $k'$  denotes the original ordering of the coded bits  $c_{k'}$  of first stream,  $k$  denotes the time ordering of the signal  $x_{1,k}$  and  $i$  indicates the position

of the bit  $c_{k'}$  in the symbol  $x_{1,k}$ . The transmission at the  $k$ -th channel use can be expressed as:-

$$\begin{aligned} \mathbf{y}_k &= \mathbf{h}_{1,k}x_{1,k} + \mathbf{h}_{2,k}x_{2,k} + \mathbf{z}_k \\ &= \mathbf{H}_k \mathbf{x}_k + \mathbf{z}_k \end{aligned} \quad (1)$$

where  $\mathbf{H}_k = [\mathbf{h}_{1,k} \ \mathbf{h}_{2,k}]$  i.e. the channel at  $k$ -th channel use and  $\mathbf{x}_k = [x_{1,k} \ x_{2,k}]^T$ . Each channel use corresponds to a symbol from a constellation map  $\chi_1$  for first stream and  $\chi_2$  for second stream.  $\mathbf{y}_k, \mathbf{z}_k \in \mathbb{C}^{n_r}$  are the vectors of received symbols and circularly symmetric complex white Gaussian noise of double-sided power spectral density  $N_0/2$  at  $n_r$  receive antennas.  $\mathbf{h}_{1,k} \in \mathbb{C}^{n_r}$  is the vector characterizing channel response from first transmitting antenna to  $n_r$  receive antennas at  $k$ -th channel use. The complex symbols  $x_{1,k}$  and  $x_{2,k}$  of two streams are assumed to be independent with variances  $\sigma_1^2$  and  $\sigma_2^2$  respectively.

**Spatial Correlation Structure.** The entries of the channel matrix are assumed to be circularly symmetric complex Gaussian random variables with zero-mean and unit variance so their magnitudes exhibit Rayleigh distribution. The average Frobenius norm is equal to  $n_r \times n_t$  (this is not the case for the instantaneous Frobenius norm).  $\mathbf{H}_k(i, j)$  is the complex path gain between  $j$ -th BS and  $i$ -th antenna of MS at  $k$ -th channel use and has the following covariance structure [5]

$$E[\mathbf{H}_k(p, j) \mathbf{H}_k(q, l)^*] = \Psi_T(j, l) \Psi_R(p, q) \quad (2)$$

where  $\Psi_R$  and  $\Psi_T$  are  $n_r \times n_r$  receive and  $n_t \times n_t$  transmit correlation matrices. The correlation matrix being Hermitian leads to orthogonal eigenvectors and being positive semidefinite leads to non-negative eigenvalues. So the square root of the correlation matrix is found by eigenvalue decomposition of the matrix [6]  $\Psi_R = \mathbf{E} \mathbf{\Lambda} \mathbf{E}^{-1}$  where  $\mathbf{E}$  is the matrix of eigenvectors and  $\mathbf{\Lambda}$  is the diagonal matrix with the eigenvalues on the diagonal. Eigenvectors being orthogonal leads to  $\Psi_R = \mathbf{E} \mathbf{\Lambda} \mathbf{E}^\dagger$  and accordingly the square root of the correlation matrix is

$$\Psi_R^{1/2} = \mathbf{E} \sqrt{\mathbf{\Lambda}} \mathbf{E}^\dagger \quad (3)$$

So  $\Psi_R = \Psi_R^{1/2} \Psi_R^{1/2} = \Psi_R^{\dagger/2} \Psi_R^{1/2} = \Psi_R^{1/2} \Psi_R^{\dagger/2}$ .

This fading model embodies following assumptions.

- The correlation between the fading from a BS to receive antenna  $j$  and to receive antenna  $l$  is  $\Psi_R(j, l)$  and does not depend on the base station.  $\Psi_R$  is equal to the correlation of  $n_r \times 1$  vector channel when excited by any BS and is therefore the same for all BSs i.e.  $\Psi_R = \frac{1}{n_t} E[\mathbf{H}_k \mathbf{H}_k^\dagger]$ .
- The correlation between fading from BSs  $p$  and  $q$  to same receive antenna at MS is  $\Psi_T(p, q)$  and does not depend on receive antenna. The transmit correlation matrix is given as  $\Psi_T = \frac{1}{n_r} E[\mathbf{H}_k^\dagger \mathbf{H}_k]$ .
- The correlation between the fading of 2 distinct antennas pairs is the product of the corresponding transmit correlation and receive correlation.
- The spatial correlation is independent of the channel use.

Each  $\mathbf{H}_k$  is spatially correlated with the correlation of  $\text{vec}(\mathbf{H}_k)$  modeled by  $\Psi_T^T \otimes \Psi_R$ . We assume the statistics to be stationary

(time invariant), therefore only one spatial correlation matrix suffices.

Let us now focus on the structure of correlation matrix. We consider single-parameter exponential correlation matrix model [7]. For this model, the components of  $\Psi_R$  are given by

$$\begin{aligned} \Psi_R(p, q) &= \rho^{\text{abs}(q-p)}, & p \leq q \\ &= \left(\rho^{\text{abs}(q-p)}\right)^*, & p > q \end{aligned}$$

where  $\rho$  is the (complex) correlation coefficient of neighboring receive branches with  $|\rho| \leq 1$ . Similarly the components of  $\Psi_T$  are given by

$$\begin{aligned} \Psi_T(j, l) &= \tau^{\text{abs}(l-j)}, & j \leq l \\ &= \left(\tau^{\text{abs}(l-j)}\right)^*, & j > l \end{aligned}$$

where  $\tau$  is the (complex) correlation coefficient of two BSs with  $|\tau| \leq 1$ . Obviously, this may not be an accurate model for some real-world scenarios but it has been shown that this model can approximate the correlation in a uniform linear array under rich scattering conditions [7] with correlation decreasing with increasing distance between the antennas.

**Temporal Correlation Structure.** An accurate model of channel variations must describe sample to sample correlation in addition to spatial correlation. For Kronecker model, temporal autocorrelation function (ACF) [8] is determined by the inverse Fourier transform of the doppler power spectrum density (PSD) i.e. when doppler PSD is U-shape, the temporal ACF between times  $t_1$  and  $t_2$  is given by the Bessel function i.e.  $J_0(2\pi v(t_2 - t_1)/\lambda)$ . where  $v$  is the velocity. In discrete domain, ACF between two channel uses  $k$  and  $k + d$  is given by  $J_0(2\pi f_d T_s d)$  where  $f_d$  is the maximum doppler frequency. Correlation between  $\mathbf{H}_k(i, j)$  and  $\mathbf{H}_{k+d}(q, l)$  has the following structure:

$$E[\mathbf{H}_k(p, j) \mathbf{H}_{k+d}(q, l)^*] = \Psi_T(j, l) \Psi_R(p, q) J_0(2\pi f_d T_s d) \quad (4)$$

where  $T_s$  is the sampling frequency. Now we define  $\mathbf{H} = [\mathbf{H}_1 \cdots \mathbf{H}_K]$  i.e. the channels for  $K$  channel uses where  $\mathbf{H}$  is  $n_r \times 2K$  matrix. Assume that the temporal correlation of the channel is modeled by a  $K \times K$  matrix  $\Psi_t$  i.e.  $\Psi_t(i, j)$  is the correlation of the channel between two channel uses  $i$  and  $j$ . Note that  $\text{vec}(\mathbf{H}^\dagger) = \Psi^{1/2} \text{vec}(\mathbf{W}^\dagger)$  where  $\mathbf{W}$  is the spatially white (Rayleigh iid) MIMO channel and  $\Psi$  is the  $K n_R n_T \times K n_R n_T$  covariance matrix defined as  $\Psi = E\{\text{vec}(\mathbf{H}) \text{vec}(\mathbf{H})^\dagger\} = \Psi_R \otimes \Psi_t \otimes \Psi_T$ . After some algebra  $\mathbf{H}$  can be modeled as

$$\mathbf{H} = \Psi_R^{1/2} \mathbf{W} (\Psi_t \otimes \Psi_T)^{T/2} \quad (5)$$

This channel matrix represents the *Kronecker correlation model* [5] since the correlation of the vectorized channel matrix can be written as the Kronecker product of transmit, receive and temporal correlation.

### III. PEP ANALYSIS - MAX LOG MAP DETECTOR

For low complexity max log MAP detection [2], the bit metric for the first stream in its full form is given as:-

$$\lambda_1^i(\mathbf{y}_k, c_{k'}) \approx \min_{x_1 \in \chi_{1,c_{k'}}, x_2 \in \chi_2} \frac{1}{N_0} \|\mathbf{y}_k - \mathbf{h}_{1,k}x_1 - \mathbf{h}_{2,k}x_2\|^2$$

where  $\chi_{1,c_{k'}}$  denotes the subset of the signal set  $x_1 \in \chi_1$  whose labels have the value  $c_{k'} \in \{0, 1\}$  in the position  $i$ .

The conditional PEP i.e.  $P(\mathbf{c}_1 \rightarrow \hat{\mathbf{c}}_1 | \bar{\mathbf{H}}) = \mathcal{P}_{\mathbf{c}_1 | \bar{\mathbf{H}}}^{\hat{\mathbf{c}}_1}$  of low complexity max log MAP detector [9] is given as:-

$$\mathcal{P}_{\mathbf{c}_1 | \bar{\mathbf{H}}}^{\hat{\mathbf{c}}_1} = P \left( \sum_{k'} \min_{x_1 \in \chi_{1,c_{k'}}, x_2 \in \chi_2} \frac{1}{N_0} \|\mathbf{y}_k - \mathbf{h}_{1,k}x_1 - \mathbf{h}_{2,k}x_2\|^2 \geq \sum_{k'} \min_{x_1 \in \chi_{1,\hat{c}_{k'}}, x_2 \in \chi_2} \frac{1}{N_0} \|\mathbf{y}_k - \mathbf{h}_{1,k}x_1 - \mathbf{h}_{2,k}x_2\|^2 \right) \quad (6)$$

where  $\bar{\mathbf{H}} = [\mathbf{H}_1 \cdots \mathbf{H}_N]$  i.e. the complete channel for the transmission of codeword  $\mathbf{c}_1$ . For the worst case scenario once  $d(\mathbf{c}_1 - \hat{\mathbf{c}}_1) = d_{free}$ , the inequality on the right hand side of (6) shares the same terms on all but  $d_{free}$  summation points for which  $\hat{c}_{k'} = \bar{c}_{k'}$  where  $(\cdot)$  denotes the binary complement. Let

$$\begin{aligned} \tilde{x}_{1,k}, \tilde{x}_{2,k} &= \arg \min_{x_1 \in \chi_{1,c_{k'}}, x_2 \in \chi_2} \frac{1}{N_0} \|\mathbf{y}_k - \mathbf{h}_{1,k}x_1 - \mathbf{h}_{2,k}x_2\|^2 \\ \hat{x}_{1,k}, \hat{x}_{2,k} &= \arg \min_{x_1 \in \chi_{1,\hat{c}_{k'}}, x_2 \in \chi_2} \frac{1}{N_0} \|\mathbf{y}_k - \mathbf{h}_{1,k}x_1 - \mathbf{h}_{2,k}x_2\|^2 \end{aligned} \quad (7)$$

As  $x_{1,k}$  and  $x_{2,k}$  are the transmitted symbols so  $\|\mathbf{y}_k - \mathbf{h}_{1,k}x_{1,k} - \mathbf{h}_{2,k}x_{2,k}\|^2 \geq \|\mathbf{y}_k - \mathbf{h}_{1,k}\tilde{x}_{1,k} - \mathbf{h}_{2,k}\tilde{x}_{2,k}\|^2$ . The conditional PEP is given as

$$\begin{aligned} \mathcal{P}_{\mathbf{c}_1 | \bar{\mathbf{H}}}^{\hat{\mathbf{c}}_1} &\leq P \left( \sum_{k, d_{free}} \frac{1}{N_0} \|\mathbf{y}_k - \mathbf{h}_{1,k}x_{1,k} - \mathbf{h}_{2,k}x_{2,k}\|^2 \geq \sum_{k, d_{free}} \frac{1}{N_0} \|\mathbf{y}_k - \mathbf{h}_{1,k}\hat{x}_{1,k} - \mathbf{h}_{2,k}\hat{x}_{2,k}\|^2 \right) \\ &= P \left( \sum_{k, d_{free}} \frac{1}{N_0} 2\Re(\mathbf{z}_k^\dagger \mathbf{H}_k (\hat{\mathbf{x}}_k - \mathbf{x}_k)) \geq \sum_{k, d_{free}} \frac{1}{N_0} \|\mathbf{H}_k \mathbf{x}_k - \mathbf{H}_k \hat{\mathbf{x}}_k\|^2 \right) \\ &= Q \left( \sqrt{\sum_{k, d_{free}} \frac{1}{2N_0} \|\mathbf{H}_k (\hat{\mathbf{x}}_k - \mathbf{x}_k)\|^2} \right) \\ &= Q \left( \sqrt{\frac{1}{2N_0} \text{vec}(\bar{\mathbf{H}}^\dagger)^\dagger \Delta \text{vec}(\bar{\mathbf{H}}^\dagger)} \right) \end{aligned} \quad (8)$$

where  $\Delta = \mathbf{I}_{n_r} \otimes \mathbf{D}\mathbf{D}^\dagger$  while  $\mathbf{D}_{2K \times K} = \text{diag}\{\hat{\mathbf{x}}_1 - \mathbf{x}_1, \hat{\mathbf{x}}_2 - \mathbf{x}_2, \dots, \hat{\mathbf{x}}_{k,d_{free}} - \mathbf{x}_{k,d_{free}}\}$  so  $\mathbf{D}\mathbf{D}^\dagger$

is a  $2K \times 2K$  block diagonal matrix with real entries on the main diagonal. Note that  $\bar{\mathbf{H}} = [\mathbf{H}_1 \cdots \mathbf{H}_K]$  where  $K = d_{free}$ . Using the Chernoff bound [8]  $Q(x) \leq \frac{1}{2} \exp\left(-\frac{x^2}{2}\right)$ , the conditional PEP can be written as:-

$$\mathcal{P}_{\mathbf{c}_1 | \bar{\mathbf{H}}}^{\hat{\mathbf{c}}_1} \leq \frac{1}{2} \exp\left(-\frac{1}{4N_0} \text{vec}(\bar{\mathbf{H}}^\dagger)^\dagger \Delta \text{vec}(\bar{\mathbf{H}}^\dagger)\right) \quad (9)$$

Note that  $\bar{\mathbf{H}} = \Psi_R^{1/2} [\mathbf{W}_1 \cdots \mathbf{W}_K] (\Psi_t \otimes \Psi_T)^{T/2} = \Psi_R^{1/2} \bar{\mathbf{W}}_{n_r \times 2K} (\Psi_t^{T/2} \otimes \Psi_T^{T/2})$ . Using the Kronecker product identity  $\text{vec}(\mathbf{A}\mathbf{X}\mathbf{B}) = (\mathbf{B}^T \otimes \mathbf{A}) \text{vec}(\mathbf{X})$  [6] we get

$$\text{vec}(\bar{\mathbf{H}}^\dagger) = (\Psi_R^{*/2} \otimes \Psi_t^{*/2} \otimes \Psi_T^{*/2}) \text{vec}(\bar{\mathbf{W}}^\dagger) \quad (10)$$

Developing (9) on the lines of [10]:-

$$\begin{aligned} \mathcal{P}_{\mathbf{c}_1 | \bar{\mathbf{H}}}^{\hat{\mathbf{c}}_1} &\leq \frac{1}{2} \exp\left(-\frac{1}{4N_0} \text{vec}(\bar{\mathbf{H}}^\dagger)^\dagger \Delta \text{vec}(\bar{\mathbf{H}}^\dagger)\right) \\ &\stackrel{a}{=} \frac{1}{2} \exp\left(-\frac{1}{4N_0} \text{vec}(\bar{\mathbf{W}}^\dagger)^\dagger (\Psi_R^{T/2} \otimes \Psi_t^{T/2} \otimes \Psi_T^{T/2}) (\mathbf{I}_{n_r} \otimes \mathbf{D}\mathbf{D}^\dagger) \right. \\ &\quad \times (\Psi_R^{*/2} \otimes \Psi_t^{*/2} \otimes \Psi_T^{*/2}) \text{vec}(\bar{\mathbf{W}}^\dagger) \left. \right) \\ &\stackrel{b}{=} \frac{1}{2} \exp\left(-\frac{1}{4N_0} \text{vec}(\bar{\mathbf{W}}^\dagger)^\dagger (\Psi_R^{T/2} \otimes \Psi_t^{T/2} \otimes \Psi_T^{T/2}) \right. \\ &\quad \times (\Psi_R^{*/2} \otimes \mathbf{D}\mathbf{D}^\dagger (\Psi_t^{*/2} \otimes \Psi_T^{*/2})) \text{vec}(\bar{\mathbf{W}}^\dagger) \left. \right) \\ &\stackrel{c}{=} \frac{1}{2} \exp\left(-\frac{1}{4N_0} \text{vec}(\bar{\mathbf{W}}^\dagger)^\dagger (\Psi_R^{T/2} \Psi_R^{*/2}) \right. \\ &\quad \otimes (\Psi_t^{T/2} \otimes \Psi_T^{T/2}) \mathbf{D}\mathbf{D}^\dagger (\Psi_t^{*/2} \otimes \Psi_T^{*/2}) \text{vec}(\bar{\mathbf{W}}^\dagger) \left. \right) \\ &\stackrel{d}{=} \frac{1}{2} \exp\left(-\frac{1}{4N_0} \text{vec}(\bar{\mathbf{W}}^\dagger)^\dagger (\Psi_R)^T \right. \\ &\quad \otimes (\Psi_t \otimes \Psi_T)^{T/2} \mathbf{D}\mathbf{D}^\dagger (\Psi_t \otimes \Psi_T)^{*/2} \text{vec}(\bar{\mathbf{W}}^\dagger) \left. \right) \\ &\stackrel{e}{=} \frac{1}{2} \exp\left(-\frac{1}{4N_0} \text{vec}(\bar{\mathbf{W}}^\dagger)^\dagger (\Psi_R)^T \otimes \mathbf{D}\mathbf{D}^\dagger (\Psi_t \otimes \Psi_T)^T \text{vec}(\bar{\mathbf{W}}^\dagger) \right) \\ &\stackrel{f}{=} \frac{1}{2} \exp\left(-\frac{1}{4N_0} \text{vec}(\bar{\mathbf{W}}^\dagger)^\dagger (\Psi_R) \otimes \mathbf{D}\mathbf{D}^\dagger (\Psi_t \otimes \Psi_T) \text{vec}(\bar{\mathbf{W}}^\dagger) \right) \end{aligned} \quad (11)$$

where in (a) we have used the identity  $(\mathbf{A} \otimes \mathbf{B})^\dagger = \mathbf{A}^\dagger \otimes \mathbf{B}^\dagger$ , in (b) and (c) we have used the identity  $(\mathbf{A} \otimes \mathbf{C})(\mathbf{B} \otimes \mathbf{D}) = \mathbf{A}\mathbf{B} \otimes \mathbf{C}\mathbf{D}$  [6]. In (d) we have used the relation  $\Psi_R^{T/2} \Psi_R^{*/2} = (\Psi_R^\dagger \Psi_R^{1/2})^T = \Psi_R^T$  where for (e) we have used the determinant identity i.e.  $\det(\mathbf{I} + \mathbf{A} \otimes \mathbf{B}\mathbf{C}) = \det(\mathbf{I} + \mathbf{A} \otimes \mathbf{C}\mathbf{B})$  which can be proved as follows.

$$\begin{aligned} \det(\mathbf{I} + \mathbf{A} \otimes \mathbf{B}\mathbf{C}) &= \det(\mathbf{I} + \mathbf{A}\mathbf{I} \otimes \mathbf{B}\mathbf{C}) \stackrel{i}{=} \det(\mathbf{I} + (\mathbf{A} \otimes \mathbf{B})(\mathbf{I} \otimes \mathbf{C})) \\ &\stackrel{ii}{=} \det(\mathbf{I} + (\mathbf{I} \otimes \mathbf{C})(\mathbf{A} \otimes \mathbf{B})) \stackrel{iii}{=} \det(\mathbf{I} + \mathbf{I}\mathbf{A} \otimes \mathbf{C}\mathbf{B}) \end{aligned} \quad (12)$$

where in (i) and (iii) we have used the same identity as in (b) while in (ii) we have used the identity  $\det(\mathbf{I} + \mathbf{A}\mathbf{B}) = \det(\mathbf{I} + \mathbf{B}\mathbf{A})$  [6].

Note that the argument of exponential in (11) is the quadratic form of a Gaussian random variable. For a Hermitian quadratic form in complex Gaussian random variable  $q = \mathbf{m}^\dagger \mathbf{A} \mathbf{m}$  where  $\mathbf{A}$  is a Hermitian matrix and column vector  $\mathbf{m}$  is a circularly symmetric complex Gaussian vector i.e.  $\mathbf{m} \sim \mathcal{N}\mathcal{C}(\boldsymbol{\mu}, \boldsymbol{\Sigma})$  with  $\boldsymbol{\mu} = E[\mathbf{m}]$  and  $\boldsymbol{\Sigma} = E[\mathbf{m}\mathbf{m}^\dagger] - \boldsymbol{\mu}\boldsymbol{\mu}^\dagger$ ,

the MGF is [11]

$$E [\exp (-t\mathbf{m}^\dagger \mathbf{A}\mathbf{m})] = \frac{\exp \left[ -t\boldsymbol{\mu}^\dagger \mathbf{A} (\mathbf{I} + t\boldsymbol{\Sigma}\mathbf{A})^{-1} \boldsymbol{\mu} \right]}{\det (\mathbf{I} + t\boldsymbol{\Sigma}\mathbf{A})} \quad (13)$$

Using the MGF, PEP is upper bounded as

$$\mathcal{P}_{\mathbf{c}_1}^{\hat{\mathbf{c}}_1} \leq \frac{1}{2 \prod_{k=1}^{2d_{free}} \prod_{l=1}^{n_r} \left( 1 + \frac{1}{4N_0} \lambda_l (\boldsymbol{\Psi}_R) \lambda_k (\mathbf{D}\mathbf{D}^\dagger (\boldsymbol{\Psi}_t \otimes \boldsymbol{\Psi}_T)) \right)} \quad (14)$$

where we have used the identity that for full rank square matrices  $\boldsymbol{\Psi}_R$  and  $\mathbf{D}\mathbf{D}^\dagger (\boldsymbol{\Psi}_t \otimes \boldsymbol{\Psi}_T)$  of size  $n_r$  and  $2d_{free}$  respectively with the eigenvalues  $\lambda_1, \dots, \lambda_{n_r}$  and  $\mu_1, \dots, \mu_{2d_{free}}$ , the eigenvalues of  $(\boldsymbol{\Psi}_R)^T \otimes \mathbf{D}\mathbf{D}^\dagger (\boldsymbol{\Psi}_t \otimes \boldsymbol{\Psi}_T)$  are

$$\lambda_l \mu_k \quad l = 1, \dots, n_r, k = 1, \dots, 2d_{free}. \quad (15)$$

Let us now assume ideal temporal case i.e. temporal correlation matrix being unity due to the effect of long interleaving depth.  $(\mathbf{D}\mathbf{D}^\dagger)_{2K \times 2K}$  is a square block diagonal matrix and its eigenvalues are

$$\lambda_k (\mathbf{D}\mathbf{D}^\dagger) = \begin{cases} \|\hat{\mathbf{x}}_k - \mathbf{x}_k\|^2 & \text{for } k = 1, \dots, d_{free} \\ 0 & \text{for } k = d_{free} + 1, \dots, 2d_{free} \end{cases}$$

As  $\text{eig} (\mathbf{A} \otimes \mathbf{B}) = \text{eig} (\mathbf{A}) \otimes \text{eig} (\mathbf{B})$ , so if  $\lambda_1 (\boldsymbol{\Psi}_T)$  and  $\lambda_2 (\boldsymbol{\Psi}_T)$  are two eigenvalues of  $\boldsymbol{\Psi}_T$  in the increasing order, then the eigenvalues of  $\mathbf{I}_K \otimes \boldsymbol{\Psi}_T$  are given as:-

$$\lambda_k (\mathbf{I}_K \otimes \boldsymbol{\Psi}_T) = \begin{cases} \lambda_1 (\boldsymbol{\Psi}_T) & \text{for } k = 1, \dots, d_{free} \\ \lambda_2 (\boldsymbol{\Psi}_T) & \text{for } k = d_{free} + 1, \dots, 2d_{free} \end{cases}$$

Let  $\mathbf{A}$  be a  $m \times n$  matrix,  $\mathbf{B}$  is  $n \times k$  with rank  $n$  and  $\mathbf{C}$  is  $l \times m$  with rank  $m$ , then as shown in [6]

$$\begin{aligned} \text{rank} (\mathbf{A}\mathbf{B}) &= \text{rank} (\mathbf{A}) \\ \text{rank} (\mathbf{C}\mathbf{A}) &= \text{rank} (\mathbf{A}) \end{aligned}$$

so  $\text{rank} (\mathbf{D}\mathbf{D}^\dagger (\mathbf{I}_K \otimes \boldsymbol{\Psi}_T)) = d_{free}$ . So the PEP is upper-bounded as

$$\begin{aligned} \mathcal{P}_{\mathbf{c}_1}^{\hat{\mathbf{c}}_1} &\leq \frac{1}{2 \prod_{k=1}^{d_{free}} \prod_{l=1}^{n_r} \left( 1 + \frac{1}{4N_0} \lambda_l (\boldsymbol{\Psi}_R) \lambda_k (\mathbf{D}\mathbf{D}^\dagger (\mathbf{I}_K \otimes \boldsymbol{\Psi}_T)) \right)} \\ &\leq \frac{1}{2} \prod_{k=1}^{d_{free}} \prod_{l=1}^{\kappa} \frac{4N_0}{\lambda_l (\boldsymbol{\Psi}_R) \lambda_k (\mathbf{D}\mathbf{D}^\dagger (\mathbf{I}_K \otimes \boldsymbol{\Psi}_T))} \\ &= \frac{1}{2} \prod_{k=1}^{d_{free}} \prod_{l=1}^{\kappa} \frac{4N_0}{\lambda_l (\boldsymbol{\Psi}_R) \theta_k \|\hat{\mathbf{x}}_k - \mathbf{x}_k\|^2} \end{aligned} \quad (16)$$

where  $\kappa = \text{rank} (\boldsymbol{\Psi}_R)$ . As per the Lemma 1 of [12]

$$\begin{aligned} \lambda_k (\mathbf{D}\mathbf{D}^\dagger (\mathbf{I}_K \otimes \boldsymbol{\Psi}_T)) &= \theta_k \lambda_k (\mathbf{D}\mathbf{D}^\dagger) \\ &= \theta_k \|\hat{\mathbf{x}}_k - \mathbf{x}_k\|^2 \end{aligned} \quad (17)$$

such that for each  $k$ , there exists a positive real number  $\theta_k$  such that  $\lambda_1 (\boldsymbol{\Psi}_T) \leq \theta_k \leq \lambda_2 (\boldsymbol{\Psi}_T)$ .

It is insightful to evaluate (16) for the special case where the antennas are uncorrelated. In this case, (16) is modified as [4]:-

$$\mathcal{P}_{\mathbf{c}_1}^{\hat{\mathbf{c}}_1} \leq \frac{1}{2} \prod_{k=1}^{d_{free}} \frac{4N_0}{\left( \|\hat{\mathbf{x}}_k - \mathbf{x}_k\|^2 \right)^{n_r}} \quad (18)$$

In the presence of only receive correlation, (16) is modified as [13]:-

$$\mathcal{P}_{\mathbf{c}_1}^{\hat{\mathbf{c}}_1} \leq \frac{1}{2} \prod_{k=1}^{d_{free}} \prod_{l=1}^{\kappa} \frac{4N_0}{\lambda_l (\boldsymbol{\Psi}_R) \|\hat{\mathbf{x}}_k - \mathbf{x}_k\|^2} \quad (19)$$

Note that  $\|\hat{\mathbf{x}}_k - \mathbf{x}_k\|^2 \geq d_{1,\min}^2 + d_{2,\min}^2$  if  $\hat{x}_{2,k} \neq x_{2,k}$  and  $\|\hat{\mathbf{x}}_k - \mathbf{x}_k\|^2 \geq d_{1,\min}^2$  if  $\hat{x}_{2,k} = x_{2,k}$ . There exists  $2^{d_{free}}$  possible vectors of  $[\hat{x}_{2,1}, \dots, \hat{x}_{2,d_{free}}]^T$  basing on the binary criteria that  $\hat{x}_{2,k}$  is equal or not equal to  $x_{2,k}$ . We call these events as  $\xi_i$  where  $i = 1, \dots, 2^{d_{free}}$ . Moreover  $P(\hat{x}_{2,k} \neq x_{2,k})$  is independent for different values of  $k$ . Consider the event  $\xi_m$  where amongst  $d_{free}$  terms of  $\|\hat{\mathbf{x}}_k - \mathbf{x}_k\|^2$ ,  $m$  terms have  $\hat{x}_{2,k} \neq x_{2,k}$ . where the probability of the event  $\xi_m$  is given as

$$P(\xi_m) = (P(\hat{x}_{2,k} \neq x_{2,k}))^m (1 - P(\hat{x}_{2,k} \neq x_{2,k}))^{d_{free} - m} \quad (20)$$

where  $P(\hat{x}_{2,k} \neq x_{2,k})$  is the uncoded probability that the output of max log MAP detector  $\hat{x}_{2,k}$  is not equal to the actual transmitted symbol  $x_{2,k}$ . Taking into account all these cases combined with their corresponding probabilities, the PEP is upper bounded as

$$\begin{aligned} \mathcal{P}_{\mathbf{c}_1}^{\hat{\mathbf{c}}_1} &\leq \frac{1}{2} \left( \frac{4N_0}{\sigma_1^2 d_{1,\min}^2} \right)^{\kappa d_{free}} \left( \prod_{l=1}^{\kappa} \frac{1}{(\lambda_l (\boldsymbol{\Psi}_R))^{d_{free}}} \right) \times \\ &\left( \sum_{j=1}^{2^{d_{free}}} \frac{P(\xi_j(m))}{\left( 1 + \frac{\sigma_2^2 d_{2,\min}^2}{\sigma_1^2 d_{1,\min}^2} \right)^{j(m)\kappa} \left( [\theta]^j(m) \right)^\kappa \left( [\theta]^j(m') \right)^\kappa} \right) \end{aligned} \quad (21)$$

where  $j(m)$  indicates the number of terms of  $\|\hat{\mathbf{x}}_k - \mathbf{x}_k\|^2$  amongst  $d_{free}$  terms, which have  $\hat{x}_{2,k} \neq x_{2,k}$ . So PEP can be written as

$$\begin{aligned} \mathcal{P}_{\mathbf{c}_1}^{\hat{\mathbf{c}}_1} &\leq \frac{1}{2} \left( \frac{4N_0}{\sigma_1^2 d_{1,\min}^2} \right)^{\kappa d_{free}} \left( \prod_{l=1}^{\kappa} \frac{1}{(\lambda_l (\boldsymbol{\Psi}_R))^{d_{free}}} \right) \left( \frac{1}{[\theta]^{d_{free}}} \right)^\kappa \times \\ &\left( \sum_{j=0}^{d_{free}} \mathbf{C}_j^{d_{free}} \frac{(P(\hat{x}_{2,k} \neq x_{2,k}))^j (1 - P(\hat{x}_{2,k} \neq x_{2,k}))^{d_{free} - j}}{\left( 1 + \frac{\sigma_2^2 d_{2,\min}^2}{\sigma_1^2 d_{1,\min}^2} \right)^{j\kappa}} \right) \end{aligned} \quad (22)$$

where  $[\theta]^{d_{free}}$  indicates the product  $\theta_1 \theta_2 \dots \theta_{d_{free}}$  and  $d_{j,\min}^2 = \sigma_j^2 \check{d}_{j,\min}^2$  with  $\check{d}_{j,\min}^2$  being the normalized minimum distance of the constellation  $\chi_j$  for  $j = \{1, 2\}$  and  $\mathbf{C}_j^{d_{free}}$  is the binomial coefficient.

Interestingly, in the case of no temporal correlation, the overall diversity depends only on the rank of  $\boldsymbol{\Psi}_R$  and  $d_{free}$  and not on the rank of  $\boldsymbol{\Psi}_T$ . However the coding gain depends both on the eigenvalues of  $\boldsymbol{\Psi}_R$  and  $\boldsymbol{\Psi}_T$ . (22) shows full diversity

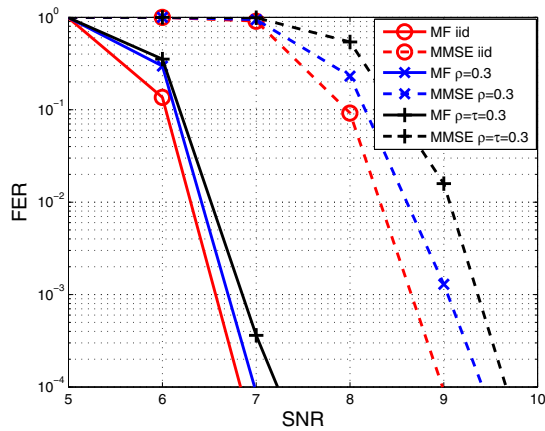


Fig. 1. Desired stream  $x_1$  is QAM16 while interference stream  $x_2$  is QPSK. Continuous lines indicate low complexity max log MAP detection while dashed lines indicate linear MMSE detection. There is no temporal correlation

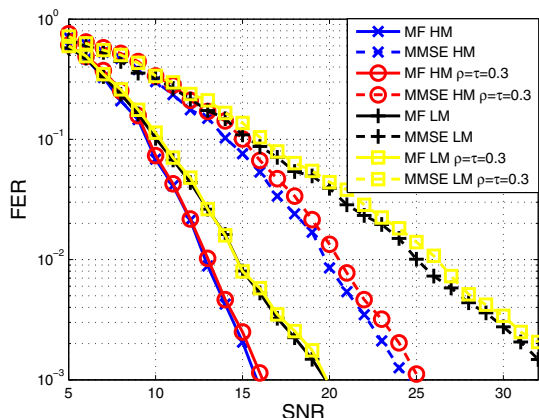


Fig. 2. Desired stream  $x_1$  is QAM16 while interference stream  $x_2$  is QPSK. HM stands for high mobility of 120km/hr while LM stands for low mobility of 10 km/hr. Both temporal and spatial correlation exist.

$(n_r \times d_{free})$  of max log MAP detector in the case of receive correlation matrix being full rank.

#### IV. SIMULATION RESULTS

We consider 2 BSs each using BICM system for downlink transmission using the punctured rate 1/2 turbo code<sup>1</sup> of 3GPP LTE [1]. We consider a narrowband MIMO system (no ISI). We assume receive diversity at the MS with two antennas. The resulting SIMO channel from BS to MS has correlated Gaussian matrix entries (receive correlation) while we also assume two SIMO channels to be correlated (transmit correlation). We also consider temporal correlation between the channel coefficients of each subchannel. For the structure of correlation matrix, we consider exponential correlation matrix model. Perfect channel state information (CSI) is assumed at

<sup>1</sup>The LTE turbo decoder design was performed using the coded modulation library [www.iterativesolutions.com](http://www.iterativesolutions.com)

the MS while BSs have no CSI. Furthermore, all mappings of coded bits to QAM symbols use Gray encoding. We consider linear MMSE detector and the low complexity max log MAP detector. Figs. 1 and 2 show the frame error rates (FERs) of desired stream for the frame size of 1056 information bits. The effects of temporal, transmit and receive correlation along with the rate of interference stream have been isolated in these simulations. To achieve this, the strengths of desired stream and interference stream are kept same (Cell Edge case) while FERs of two detectors have been approximately equated once there is no spatial or temporal correlation. Then as spatial correlation (both transmit and receive) for different scenarios of temporal correlation get stronger, the degrading effect on the performance of both the detectors in the presence of different interferences is compared. In the case of equal rate streams, the degrading effect of correlation on MMSE and low complexity max log MAP detection is approximately same. However once the interference has lower rate compared to the desired stream, the degrading effect of enhanced correlation is quite reduced on max log MAP detector as compared to MMSE detector. The degradation of MMSE performance with increase in transmit and receive correlation is independent of the rate of interference. The SNR gap between the max log MAP detection and MMSE detection for the same FER (at zero correlation) widens as rate of interference stream decreases relative to the desired stream. This can be attributed to the ability of max log MAP detector to partially decode interference once the lower rate or the higher strength of interference permits its partial decoding [4]. This partial decoding capability of max log MAP detector reduces with increased correlation especially once interference has comparable rate relative to the desired stream.

#### V. CONCLUSIONS

We have focused in this paper on the effects of temporal and spatial correlation and interference rate on the performance of low complexity max log MAP detector. We have shown that the degrading effect of correlation is less pronounced for max log MAP detector as compared to MMSE detector in the case when interference because of its relative rate allows its partial decoding. Simulations show that the degradation of MMSE performance with enhanced correlation is independent of the rate of interference.

#### ACKNOWLEDGMENTS

Eurecom's research is partially supported by its industrial partners: BMW, Bouygues Telecom, Cisco Systems, France Télécom, Hitachi Europe, SFR, Sharp, ST Microelectronics, Swisscom, Thales. The research work leading to this paper has also been partially supported by the European Commission under the IST FP7 research network of excellence NEWCOM++.

#### APPENDIX

$\mathbf{P}(\hat{x}_{2,k} \neq x_{2,k})$   
Considering the definition of  $\hat{x}_{2,k}$  in (7), it can be expanded

as:-

$$\hat{x}_{2,k} = \arg \min_{x_1 \in \mathcal{X}_{1,\hat{\epsilon}}, x_2 \in \mathcal{X}_2} \left[ \frac{1}{N_0} \left\{ \|\mathbf{h}_{1,k}(x_{1,k}-x_1) + \mathbf{z}_k\|^2 + \|\mathbf{h}_{2,k}(x_{2,k}-x_2)\|^2 + 2\Re(\mathbf{h}_{1,k}(x_{1,k}-x_1) + \mathbf{z}_k)^\dagger \mathbf{h}_{2,k}(x_{2,k}-x_2) \right\} \right]$$

The last two terms will be zero if  $\hat{x}_{2,k} = x_{2,k}$ . Conditioning it on  $x_1$ , the probability  $P(\hat{x}_{2,k} \neq x_{2,k} | \mathbf{h}_{1,k}, \mathbf{h}_{2,k}, x_1) = \mathcal{P}_{x_2 | \mathbf{H}_k, x_1}^{\hat{x}_2}$  is given as:-

$$\begin{aligned} &= P\left(-2\Re\left(\mathbf{h}_{1,k}X_{1,k} + \mathbf{z}_k\right)^\dagger \mathbf{h}_{2,k}X_{2,k}\right) \geq \|\mathbf{h}_{2,k}X_{2,k}\|^2 | \mathbf{H}_k, x_{1,k} \\ &= Q\left(\sqrt{\frac{\|\mathbf{h}_{2,k}X_{2,k}\|^2}{2N_0}} + \sqrt{\frac{2}{N_0}} \Re\left(\frac{\mathbf{h}_{1,k}X_{1,k} + \mathbf{z}_k}{\sqrt{\|\mathbf{h}_{2,k}X_{2,k}\|^2}}\right)\right) \end{aligned}$$

where  $X_{j,k}$  denotes  $(x_{j,k} - x_j)$ . Using the relation  $Q(a+b) \leq Q(a_{\min} - |b_{\max}|)$  and  $\Re(\mathbf{a}^\dagger \hat{\mathbf{b}}) \leq \|\mathbf{a}\|$  where  $\hat{\mathbf{b}}$  is the unit vector we get

$$\begin{aligned} \mathcal{P}_{x_2 | \mathbf{H}_k}^{\hat{x}_2} &\leq \frac{1}{2} \exp\left(-\frac{\|\mathbf{h}_{2,k}\|^2 d_{2,\min}^2}{4N_0} - \frac{\|\mathbf{h}_{1,k}\|^2 d_{1,\max}^2}{N_0}\right) \\ &\quad + \frac{\|\mathbf{h}_{2,k}\| \|\mathbf{h}_{1,k}\| d_{2,\min} d_{1,\max}}{N_0} \end{aligned} \quad (23)$$

Considering the norms of  $\mathbf{h}_{1,k}$  and  $\mathbf{h}_{2,k}$  we make two non-overlapping regions as  $(\|\mathbf{h}_{2,k}\| \geq \|\mathbf{h}_{1,k}\|)$  and  $(\|\mathbf{h}_{2,k}\| < \|\mathbf{h}_{1,k}\|)$  with the corresponding probabilities as  $\mathcal{P}_{\mathbf{h}_1}^<$  and  $\mathcal{P}_{\mathbf{h}_1}^>$ . Note that in the first region  $\|\mathbf{h}_{2,k}\| \|\mathbf{h}_{1,k}\| \leq \|\mathbf{h}_{2,k}\|^2$  while for second region  $\|\mathbf{h}_{2,k}\| \|\mathbf{h}_{1,k}\| < \|\mathbf{h}_{1,k}\|^2$ . So

$$\begin{aligned} \mathcal{P}_{x_2 | \mathbf{H}_k}^{\hat{x}_2} &\leq \\ &\frac{1}{2} \left[ \exp\left(-\|\mathbf{h}_{2,k}\|^2 \frac{d_{2,\min}^2 - 4d_{2,\min}d_{1,\max}}{4N_0}\right) \exp\left(-\frac{\|\mathbf{h}_{1,k}\|^2 d_{1,\max}^2}{N_0}\right) \mathcal{P}_{\mathbf{h}_1}^< \right. \\ &\quad \left. + \exp\left(-\frac{\|\mathbf{h}_{2,k}\|^2 d_{2,\min}^2}{4N_0}\right) \exp\left(-\frac{\|\mathbf{h}_{1,k}\|^2 d_{1,\max}^2 - d_{2,\min}d_{1,\max}}{N_0}\right) \mathcal{P}_{\mathbf{h}_1}^> \right] \end{aligned} \quad (24)$$

We upperbound both the probabilities i.e.  $\mathcal{P}_{\mathbf{h}_1}^<$  and  $\mathcal{P}_{\mathbf{h}_1}^>$  by 1. Taking expectation over  $\mathbf{h}_{2,k}$  conditioned on  $\mathbf{h}_{1,k}$  and then subsequently taking expectation over  $\mathbf{h}_{1,k}$  yields:-

$$\begin{aligned} \mathcal{P}_{x_2}^{\hat{x}_2} &\leq \frac{1}{2} E_{\mathbf{h}_1} \left[ \left( \frac{4N_0}{d_{2,\min}^2 - 4d_{2,\min}d_{1,\max}} \right)^\kappa \exp\left(-\frac{\|\mathbf{h}_{1,k}\|^2 d_{1,\max}^2}{N_0}\right) \prod_{l=1}^\kappa \frac{1}{\lambda_l(\Psi_R)} \right. \\ &\quad \left. + \left( \frac{4N_0}{d_{2,\min}^2} \right)^\kappa \exp\left(-\|\mathbf{h}_{1,k}\|^2 \frac{d_{1,\max}^2 - d_{2,\min}d_{1,\max}}{N_0}\right) \prod_{l=1}^\kappa \frac{1}{\lambda_l(\Psi_R)} \right] \\ &\leq \frac{1}{2} \left( \frac{4N_0}{\sigma_2^2 d_{2,\min}^2} \right)^\kappa \left( \frac{N_0}{\sigma_1^2 d_{1,\max}^2} \right)^\kappa \prod_{l=1}^\kappa \frac{1}{(\lambda_l(\Psi_R))^2} \times \\ &\quad \left( \frac{1}{\left(1 - \frac{4\sigma_1 d_{1,\max}}{\sigma_2 d_{2,\min}}\right)^\kappa} + \frac{1}{\left(1 - \frac{\sigma_2 d_{2,\min}}{\sigma_1 d_{1,\max}}\right)^\kappa} \right) \end{aligned} \quad (25)$$

where we have used the MGF of (13) while writing  $\|\mathbf{h}_{j,k}\|^2 = \mathbf{h}_{j,k}^\dagger \mathbf{I}_{n_r} \mathbf{h}_{j,k}$  where  $\mathbf{h}_{j,k} \sim \mathcal{CN}(\mathbf{0}, \Psi_R)$ . Interestingly transmit correlation being between  $\mathbf{h}_{1,k}$  and  $\mathbf{h}_{2,k}$  does not appear in the above expression. This expression shows the dependence of  $P(\hat{x}_{2,k} \neq x_{2,k})$  on the interference strength, SNR and the correlation.

## REFERENCES

- [1] LTE, *Requirements for Evolved UTRA (E-UTRA) and Evolved UTRAN (E-UTRAN)*. 3GPP TR 25.913 v.7.3.0, 2006.
- [2] R. Ghaffar and R. Knopp, "Interference Suppression for Next Generation Wireless Systems," in *IEEE 69-th Vehicular Technology Conference VTC-Spring 2009*, Barcelona, Apr. 2009.
- [3] G. Caire, G. Taricco, and E. Biglieri, "Bit-interleaved coded modulation," *IEEE Transactions on Information Theory*, vol. 44, no. 3, pp. 927-946, May 1998.
- [4] R. Ghaffar and R. Knopp, "Spatial Interference Cancellation and Pairwise Error Probability Analysis," in *IEEE International Conference on Communications, ICC 2009*, June 2009.
- [5] C. Oestges, "Validity of the kronecker model for MIMO correlated channels," in *VTC Spring, 2006*, pp. 2818-2822.
- [6] R. A. Horn and C. R. Johnson, *Matrix Analysis*. Cambridge University Press, 1985.
- [7] S. Loyka, "Channel capacity of MIMO architecture using the exponential correlation matrix," *IEEE Communications Letters*, vol. 5, no. 9, pp. 369-371, Sep 2001.
- [8] D. Tse and P. Viswanath, *Fundamentals of Wireless Communication*. Cambridge University Press, U.K, 2005.
- [9] E. Akay and E. Ayanoglu, "Achieving full frequency and space diversity in wireless systems via BICM, OFDM, STBC, and viterbi decoding," *Communications, IEEE Transactions on*, vol. 54, no. 12, pp. 2164-2172, dec. 2006.
- [10] A. Hedayat, H. Shah, and A. Nosratinia, "Analysis of space-time coding in correlated fading channels," *IEEE Transactions on Wireless Communications*, vol. 4, no. 6, pp. 2882-2891, 2005.
- [11] G. L. Turin, "The characteristic function of Hermitian quadratic forms in complex normal variables," in *Biometrika*, 1960, pp. 199-201.
- [12] H. Bolcskei and A. J. Paulraj, "Performance of spacetime codes in the presence of spatial fading correlation," in *Asilomar Conference on Signals, Systems and Computers, 2000*, pp. 687-693.
- [13] R. Ghaffar and R. Knopp, "Analysis of low complexity max log MAP detector and MMSE detector for interference suppression in correlated fading," in *IEEE Global Telecommunications Conference, IEEE Globecom 2009*, Dec 2009.